



Growth and characterization of perovskite LaGaO_3 crystals doped with Sr and Mn

M. Glowacki^{a,*}, T. Runka^b, V. Domukhovski^a, R. Diduszko^{a,c}, M. Mirkowska^c,
M. Berkowski^a, B. Dabrowski^d

^a Institute of Physics Polish Academy of Sciences, Warsaw, Poland

^b Faculty of Technical Physics, Poznan University of Technology, Poznan, Poland

^c Institute of Electronic Materials Technology, Warsaw, Poland

^d Physics Department, Northern Illinois University, DeKalb, IL 60115, USA

ARTICLE INFO

Article history:

Received 22 March 2010

Received in revised form

27 September 2010

Accepted 11 October 2010

Available online 23 October 2010

PACS:

81.10.Fq

61.50.-f

74.62.Bf

Keywords:

Oxide materials SOFCs

Crystal growth

Crystal structure

Phase transitions

Thermal analysis

X-ray diffraction

ABSTRACT

Single crystals of LaGaO_3 doped with Sr and Mn (LSGMn) were grown by the Czochralski method from the melt with compositions: $\text{La}_{1-x}\text{Sr}_x\text{Ga}_{1-y}\text{Mn}_y\text{O}_3$, $x = y = 0.02$; 0.05 and $x = 0.05$, $y = 0.06$. Single crystals with 20 mm diameter with convex crystal–melt interface were grown on LaGaO_3 oriented seed with pulling rate of 2 mm/h. Single crystals were dark and have strong tendency to spiral growth. This tendency was decreased with increasing the Mn content in comparison with Sr. Effective segregation coefficients for Sr and Mn in LaGaO_3 are lower than 1. Room-temperature structural measurements by X-ray powder diffraction showed perovskite structure with $Pbnm$ space group for all measured samples. Orthorhombic b and c lattice parameters decrease, whereas a slightly increases with decreasing orthorhombic unit cell volume that is related to increased amount of Mn and Sr in the melt. Thermal analysis and Raman investigations showed that the temperature of the first order phase transitions temperature from orthorhombic to rhombohedral structure observed in pure LaGaO_3 at about 150°C decreases to about 49°C at the bottom part of crystal with $x = y = 0.05$ composition.

© 2010 Elsevier B.V. All rights reserved.

1. Introduction

Perovskite materials have been widely studied due their extraordinary electronic and ionic conductivity and a wide range of magnetic, ferroelectric, piezoelectric, non-linear optical and other functional properties. The unit cell of the ideal undistorted ABO_3 perovskite may be described as a cube with the larger, twelve coordinated A cations at the corners, smaller, six-coordinated B cations at the center and the oxygen ions occupying centers of the cube faces. In many perovskites the ionic sizes of A , B and O ions do not match the ideal sizes and the lattice undergoes distortion. With a decrease of ionic size of the A and/or an increase of the ionic size of B the BO_6 octahedra become rotated and deformed, causing lowering of the crystal symmetry, typically from cubic through tetragonal or rhombohedral to the orthorhombic. These symmetry changes can

be readily observed and the structures achieved by chemical substitutions on the A and B sites as long as the cation sizes are acceptable and the rules of electroneutrality are satisfied.

Single crystals of gallate rare earth perovskites are suitable as substrates for epitaxial thin film deposition due to their chemical stability and tunable lattice parameters. However, their use is limited because of a strong tendency for twin formation [1,2]. The cause of twinning is the first order phase transition from orthorhombic to rhombohedral (O/R) structure, which occurs on heating near 423 K (150°C) for LaGaO_3 . Isomorphic substitution of La by smaller rare earth ions increases the O/R phase transition temperature by ca. 220 K with a change of the average RE cation radius by 0.01 \AA (for example to 1420°C for $\text{La}_{0.38}\text{Nd}_{0.62}\text{GaO}_3$), and enhances distortion of the perovskite unit cell [3–5]. Heterovalent substitution of La by larger Sr decreases the O/R phase transition temperature nonlinearly with Sr concentration to about 380 K (107°C) at 4% of Sr [5,6]. On the other hand the co-substitution of heterovalent La by at 5% of Sr and Ga by 10% of Mg increases transition temperature and induces three phase transitions at higher temperatures:

* Corresponding author.

E-mail address: glowacki@ifpan.edu.pl (M. Glowacki).

orthorhombic to monoclinic at 520–570 K, monoclinic to rhombohedral at 720 K and rhombohedral (R3c) to rhombohedral (R-3c) at ca 870 K [7].

Recently, lanthanum gallate co-doped with fix-oxidation state Sr and Mg (LSGM) has been extensively investigated as electrolyte material for intermediate temperature solid oxide fuel cells (SOFC) due to their high and stable oxide-ion conductivity [8,9]. The most widely used anode material containing Ni is prone to react with an LSGM electrolyte to form a lanthanum-nickel oxide. This surface reaction blocks the O^{2-} ion transport needed for the fuel-cell reaction [8]. Further research on LSGM single crystals showed that changes of the slope of the conductivity versus temperature curves coincide with the structural transitions and thermal expansion anomalies [7]. Lanthanum gallates co-doped with Sr and Mn or other transition metal elements are considered as good candidates for anode materials based on LSGM electrolyte SOFC [10,11]. They are chemically and physically compatible with LSGM electrolytes minimizing thus interfacial reactions, and have thermal expansion coefficients similar to that of LSGM. It was also shown [10] that LSGMn anode with higher Mn content exhibited far superior performance than that with lower Mn content.

The $SrMnO_3$ is a cubic perovskite over entire temperature range due to large and small ionic sizes of the Sr and Mn ions, respectively [12]. It is expected thus that the electroneutral Sr and Mn co-doped $LaGaO_3$ (LSGMn) should exhibit decreased temperatures of the phase transition from orthorhombic to rhombohedral structure. This lowering of the O/R phase transition temperatures intended for improved thin films substrates, as well as compatibility with the LSGM electrolytes makes LSGMn interesting for in-depth investigation. In the present paper we report our initial study of the growth conditions, structure and phase transition for LSGMn single crystals and compare them with similar work on other substituted lanthanum gallates.

2. Experimental procedures

Single crystals of $LaGaO_3$ co-doped with Sr and Mn were grown by the Czochralski method from the melt with compositions: $La_{1-x}Sr_xGa_{1-y}Mn_yO_3$ where $x = y = 0.02$; 0.05 and $x = 0.05$, $y = 0.06$. Starting materials (La_2O_3 , Ga_2O_3) were heated at 1000 °C and ($SrCO_3$, MnO_2) at 300 °C for 6 h before mixing in stoichiometric ratios and melting in 40 mm iridium crucible. Single crystals with 20 mm diameter with convex crystal–melt interface were grown on (1 0 0) $LaGaO_3$ oriented seed with pulling rate of 2 mm/h and a rotation of 20 rpm. Crystals were grown under ambient pressure in a nitrogen atmosphere containing 1 vol.% of oxygen. Single crystals were dark and have strong tendency to spiral growth, especially the one with $x = y = 0.05$. This tendency to spiral growth was decreased with increasing the Mn content ($x = 0.05$, $y = 0.06$). Samples compositions were determined with a ARL – 8600 s – Wavelength Dispersive X-ray Fluorescence Spectrometer. It was found that the Sr and Mn concentrations increase along the growth direction of crystals indicating that the effective segregation coefficients for Sr and Mn are lower than 1 in $LaGaO_3$ matrix.

Samples for structural and DSC measurements were prepared from top and bottom parts of crystals with $La_{1-x}Sr_xGa_{1-y}Mn_yO_3$ compositions $x = y = 0.02$ and 0.05. Sample for Raman spectroscopy measurements was prepared from the central part of $x = 0.05$, $y = 0.06$ crystal.

3. Structure analyses

Structure analyses of prepared samples was performed by X-ray powder diffraction using Ni-filtered $Cu K\alpha$ radiation with a Siemens D5000 diffractometer after grinding small parts of crystal. Data were collected in the angle range $20^\circ < 2\theta < 140^\circ$ with a step 0.02° and the averaging time of 10 s/step. The diffraction patterns were analyzed by the Rietveld refinement method in space group $Pbnm$. Room-temperature XRD measurements showed perovskite-like structure for all measured samples. Differences between diffraction and simulation patterns and some unidentified reflections visible on diffraction spectra shown on Fig. 1 are caused by pref-

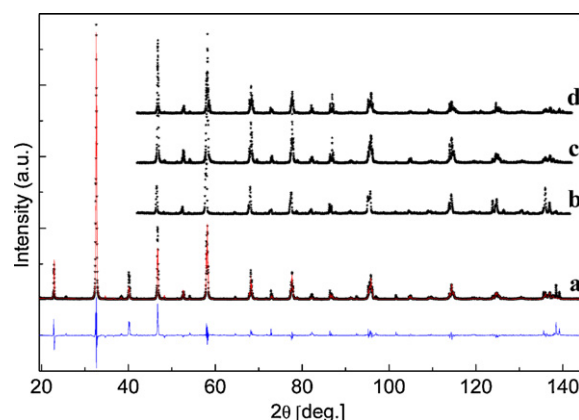


Fig. 1. Diffraction patterns and Rietveld refinements for $La_{1-x}Sr_xGa_{1-y}Mn_yO_3$ crystals grown from the melt with the following compositions: a) top part of crystal with $x = y = 0.02$; b) bottom part of crystal with $x = y = 0.02$; c) top part of crystal with $x = y = 0.05$; d) bottom part of crystal with $x = y = 0.05$.

erential orientation and presence of small amounts of impurity phases.

The refinement procedure showed a quite good fit between experimental and calculated profiles. Fig. 1 shows graphical result of the Rietveld refinement for the sample cut from top part of $La_{1-x}Sr_xGa_{1-y}Mn_yO_3$ crystal with $x = y = 0.02$ compared to other diffraction patterns of LSGMn crystals cut from bottom part of crystal grown from the melt with $x = y = 0.02$ and top and bottom part of crystal grown from the melt with $x = y = 0.05$. The orthorhombic unit cell parameters of $LaGaO_3$ single crystal for all measured samples are listed in Table 1. It follows from the results that the b and c lattice parameters of $La_{1-x}Sr_xGa_{1-y}Mn_yO_3$ crystals decrease, whereas a slightly increases resulting in decreasing orthorhombic unit cell volume that is related to increased amount of Mn and Sr in the melt. This result is consistent with lattice parameters changes in $La_{1-x}Sr_xGaO_3$ crystals [6] and $La_{1-x}Sr_xMnO_3$ [13]. Kuscer et al. showed also that the volume for $La_{1-x}Sr_xMnO_3$ at first increases as a consequence of cation vacancy disappearance, until $x = 0.1$. After that, the unit-cell volume decreases linearly with increasing Sr content as a result of Mn^{4+} formation [14]. Different behavior of lattice parameters is observed in $La_{1-x}Sr_xGa_{1-y}Mg_yO_3$ crystals for which increased amount of dopant enlarges the unit cell volume, which is expected because both Sr^{2+} and Mg^{2+} ions are bigger than La^{3+} and Ga^{3+} ions, respectively [15,16]. Observed decrease of unit cell volume vs. Sr and Mn content in $La_{1-x}Sr_xGa_{1-y}Mn_yO_3$ crystals is most probably a superposition of two mechanisms—enlargement with Sr content ($r(Sr^{2+})$ 1.44 Å > $r(La^{3+})$ 1.36 Å) and contraction with Mn content ($r(Mn^{4+})$ 0.53 Å < $r(Ga^{3+})$ 0.62 Å); ionic radii according to [17]. Considering that ionic radius of Mn^{3+} (0.645 Å) is larger than Ga this indicates that Mn exists in charge state close to 4+ in $La_{1-x}Sr_xGa_{1-y}Mn_yO_3$ crystals. Precise studies of the average formal valence of Mn and the oxygen content based on thermogravimetric and x-ray absorption spectroscopy will be shown elsewhere.

Table 1

Crystallographic data for the RT structures of $La_{1-x}Sr_xGa_{1-y}Mn_yO_3$ crystals.

LSGMn crystal x and y in the melt	a_{ort} [Å]	b_{ort} [Å]	c_{ort} [Å]	V [Å ³]
$x = y = 0$	5.5237	5.4918	7.7732	235.81
$x = y = 0.02$ top	5.5241	5.4906	7.7717	235.72
$x = y = 0.02$ bottom	5.5247	5.4906	7.7707	235.72
$x = y = 0.05$ top	5.5252	5.4878	7.7701	235.60
$x = 0.05$ $y = 0.06$	5.5248	5.4881	7.7695	235.58
$x = y = 0.05$ bottom	5.5250	5.4877	7.7672	235.49

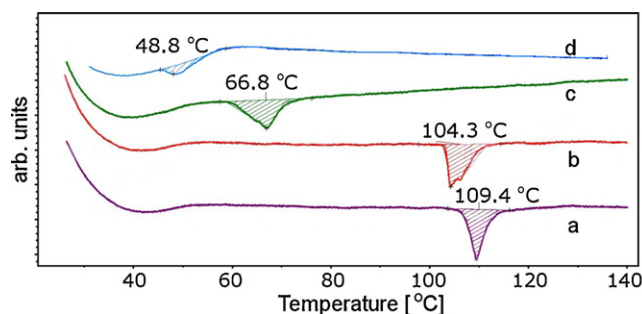


Fig. 2. DSC measurements of $\text{La}_{1-x}\text{Sr}_x\text{Ga}_{1-y}\text{Mn}_y\text{O}_3$ crystals with $x=y=0.02$ in the melt a) top and b) bottom parts. Measurements for crystal with $x=y=0.05$ in the melt c) top and d) bottom of crystal.

4. Thermal analyses and Raman spectroscopy

Preliminary thermal behavior was studied by using simultaneous calorimetric and thermogravimetric measurements on DSC-TG (STA 449 F1 Jupiter, Netzsch). Samples were heated from 300 to 420 K with heating rate of 2 K/min in argon atmosphere. In pure LaGaO_3 structural O/R phase transition from orthorhombic $Pbnm$ to rhombohedral $R-3c$ is observed at $\sim 150^\circ\text{C}$. DSC measurements (Fig. 2) and Raman spectroscopy (Figs. 3 and 4) showed such phase transition also in $\text{La}_{1-x}\text{Sr}_x\text{Ga}_{1-y}\text{Mn}_y\text{O}_3$ crystals (DSC measurements for $x=y=0.02$ and 0.05, Raman spectroscopy for $x=0.05$, $y=0.06$).

The Raman investigations of $\text{La}_{1-x}\text{Sr}_x\text{Ga}_{1-y}\text{Mn}_y\text{O}_3$ crystal with $x=0.05$ and $y=0.06$ were performed in $X(\text{ZY})\bar{X}$ back-scattering geometry using Renishaw InVia Raman microscope equipped with a thermoelectrically (TE)-cooled RenCam CCD detector and Ar^+ ion laser working at 488 nm wavelength. The polarized Raman spectra were measured in the $100\text{--}900\text{ cm}^{-1}$ spectral range. In order to avoid locally heating the sample the applied power of the laser beam was less than 0.7 mW before focusing with $\times 50$ long working distance objective (LWD). An Edge filter was used to stray Rayleigh light rejection. The instrumental resolution was better than 2 cm^{-1} . The position of Raman peaks was calibrated before collecting the data using Si sample as an internal standard.

The temperature measurements were performed using Linkam THMS 600 cooling/heating stage in temperature range $56\text{--}69^\circ\text{C}$ with 0.5 or 1°C step and temperature stability of 0.1°C . The temperature-dependent Raman spectra were fitted using spectral

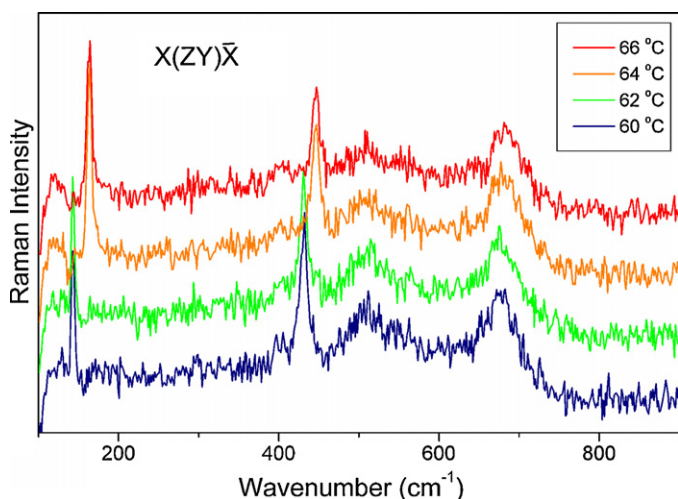


Fig. 3. Raman spectra of oriented $\text{La}_{1-x}\text{Sr}_x\text{Ga}_{1-y}\text{Mn}_y\text{O}_3$ crystal (with $x=0.05$ and $y=0.06$) below and above the structural phase transition at 63°C .

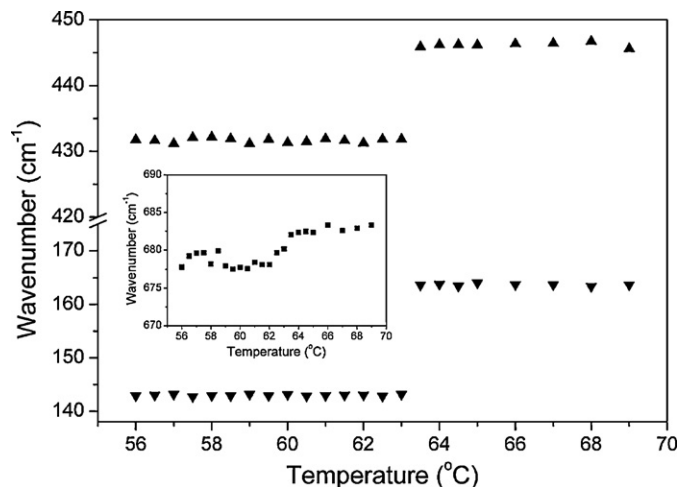


Fig. 4. Temperature dependence of the wave number of Raman modes attributed to in-plane La and O shifts and La-O stretching vibrations of the central part of $\text{La}_{1-x}\text{Sr}_x\text{Ga}_{1-y}\text{Mn}_y\text{O}_3$ crystal with $x=0.05$ and $y=0.06$ in the melt.

response function: $S(\nu) = S_0(\nu)[n(\nu) + 1]$, where $n(\nu) = (e^{h\nu/kT} - 1)^{-1}$ is the Bose-Einstein population factor. The temperature evolution of Raman spectra in the vicinity of the phase transition at about 63°C is presented in Fig. 3.

The main changes in Raman spectra have been observed in the spectral range $140\text{--}165\text{ cm}^{-1}$ and $430\text{--}450\text{ cm}^{-1}$. The Raman modes occurring in the first range are attributed to lattice vibrations, mainly the in-plane La and O shifts, while modes corresponding to the second range are mainly assigned to La-O stretching vibrations [18]. The wavenumber discontinuities of these modes are presented in Fig. 4. The anomaly of the wavenumber of other modes detected in the spectra, that assigned to internal vibrations of MnO_6 octahedra e.g., stretching vibrations at about 680 cm^{-1} were also observed (inset of Fig. 4) [19–21].

The O/R phase transition temperature decreases from 148.5°C to 48.8°C with decreasing size of the orthorhombic unit cell volume that is related to increased amount of Mn and Sr in the melt. The dependence of the O/R phase transition temperature and normalized lattice parameters $a_n = a_{\text{ort}}/\sqrt{2}$; $b_n = b_{\text{ort}}/\sqrt{2}$; $c_n = c_{\text{ort}}/2$ on the size of orthorhombic unit cell volume are presented in Fig. 5.

Similar dependence of the O/R phase transition temperature on dopant concentration was observed in $\text{La}_{1-x}\text{Sr}_x\text{GaO}_3$ and $\text{La}_{1-x}\text{Sr}_x\text{MnO}_3$ crystals, however lowest obtained O/R phase transition temperature in $\text{La}_{1-x}\text{Sr}_x\text{GaO}_3$ was about 380 K (107°C) at 4%

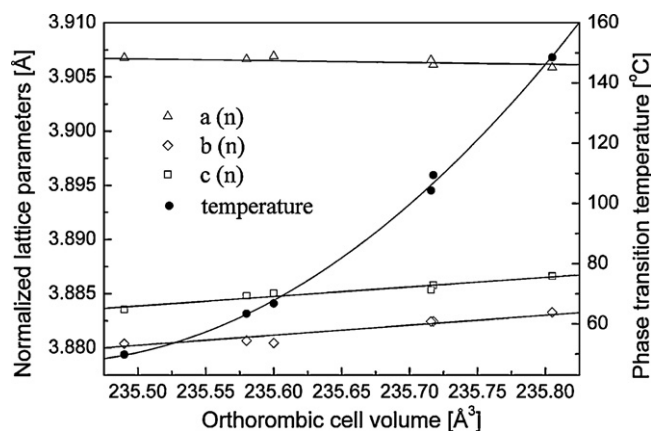


Fig. 5. Dependence of normalized lattice parameters $a_n = a_{\text{ort}}/\sqrt{2}$; $b_n = b_{\text{ort}}/\sqrt{2}$; $c_n = c_{\text{ort}}/2$ and temperatures of the first order phase transition on orthorhombic unit cell volume.

of Sr [6], which is much higher than 322 K ($\sim 49^\circ\text{C}$) in LSGMn. In $\text{La}_{1-x}\text{Sr}_x\text{MnO}_3$ O/R phase transition was observed at 360 K [22] and at room temperature [23] in crystals with much higher Sr concentration (15% and 17.5% of Sr respectively).

5. Conclusions

Single crystals of LaGaO_3 doped with Sr and Mn were grown by the Czochralski method. Crystals were dark and have strong tendency to spiral growth, which increases with increasing of Sr and Mn concentration. Tendency to spiral growth decreases when Mn content in the melt is higher than Sr. Effective segregation coefficients for Sr and Mn in LaGaO_3 are different but both are lower than 1. With increasing of Sr and Mn concentration in LSGMn crystals the orthorhombic unit cell volume decreases and simultaneously lattice parameter a increase slightly, whereas b and c decrease.

Heterovalent substitution of La by Sr in LaGaO_3 crystals was previously observed to decrease the O/R phase transition temperature and increase the orthorhombic unit cell volume. Co-substitution of La and Ga by Sr and Mg, respectively, increase the O/R phase transitions temperature and decrease the orthorhombic unit cell volume. In $\text{La}_{1-x}\text{Sr}_x\text{Ga}_{1-y}\text{Mn}_y\text{O}_3$ crystals with $x=y$ from 0 to 0.05 studied here the substitutions of La and Ga by Sr and Mn, respectively, decrease the orthorhombic unit cell volume and causes expected decrease of the O/R phase transition temperature to about 49°C . It is interesting to note that both deviation from the ideal cubic perovskite structure and orthorhombic unit cell volume decrease with increasing Sr and Mn concentration in these crystals.

Acknowledgement

Work at NIU was supported by the NSF-DMR-0706610.

References

- [1] M. Kurumada, E. Iguchi, D.I. Savvitskii, J. Appl. Phys. 100 (2006) 014107.
- [2] D.I. Savvitskii, D.M. Trots, L.O. Vasylechko, N. Tamura, M. Berkowski, J. Appl. Crystallogr. 36 (2003) 1197–1203.
- [3] M. Berkowski, J. Fink-Finowicki, W. Piekarczyk, L. Perchuc, P. Byszewski, L.O. Vasylechko, D.I. Savvitskij, K. Mazur, J. Sass, E. Kowalska, J. Kapusniak, J. Cryst. Growth 209 (2000) 75–80.
- [4] L. Vasylechko, R. Niewa, H. Borrmann, M. Knapp, D. Savvitskii, A. Matkovski, U. Bismayer, M. Berkowski, Solid State Ionics 143 (2001) 219–227.
- [5] R. Aleksieyko, M. Berkowski, P. Byszewski, B. Dabrowski, R. Diduszko, J. Fink-Finowicki, L.O. Vasylechko, Cryst. Res. Technol. 36 (2001) 789–800.
- [6] R. Aleksieyko, M. Berkowski, J. Fink-Finowicki, P. Byszewski, R. Diduszko, E. Kowalska, Proc. SPIE 4412 (2001) 50–54.
- [7] L. Vasylechko, V. Vashook, D. Savvitskii, A. Senyshyn, R. Niewa, M. Knapp, H. Ullmann, M. Berkowski, A. Matkovskii, U. Bismayer, J. Solid State Chem. 172 (2003) 396–411.
- [8] K. Huang, J.B. Goodenough, J. Alloys Compd. 303–304 (2000) 454–464.
- [9] B.C.H. Steele, A. Heinzel, Nature 414 (2001) 345–352.
- [10] Q. Fu, X. Xu, D. Peng, X. Liu, G. Meng, J. Mater. Sci. 38 (2003) 2901–2906.
- [11] N. Trofimenko, H. Ullmann, Solid State Ionics 118 (1999) 215–227.
- [12] O. Chmaissem, B. Dabrowski, S. Kolesnik, J. Mais, D.E. Brown, R. Kruk, P. Prior, B. Pyles, J.D. Jorgensen, Phys. Rev. B 64 (2001) 134412.
- [13] W.H. McCarroll, K.V. Ramanujachary, I.D. Fawcett, M. Greenblatt, J. Solid State Chem. 145 (1999) 88–96.
- [14] D. Kuscer, M. Hrovat, J. Holc, S. Bernik, D. Kolar, Mater. Res. Bull. 35 (2000) 2525–2544.
- [15] P. Datta, P. Majewski, F. Aldinger, J. Alloys Compd. 438 (2007) 232–237.
- [16] H. Inaba, H. Hayashi, M. Suzuki, Solid State Ionics 144 (2001) 99–108.
- [17] R.D. Shannon, Acta Crystallogr. A 32 (1976) 751–767.
- [18] M.L. Sanjuán, V.M. Orera, R.I. Merino, J. Blasco, J. Phys.: Condens. Matter 10 (1998) 11687.
- [19] M. Baldini, D. Di Castro, M. Cestelli-Guidi, J. Garcia, P. Postorino, Phys. Rev. B 80 (2009) 045123–45131.
- [20] L. Martín-Carrón, A. de Andrés, M.J. Martínez-Lope, M.T. Casais, J.A. Alonso, Phys. Rev. B 66 (2002) 174303.
- [21] M.N. Iliev, M.V. Abrashev, H.-G. Lee, V.N. Popov, Y.Y. Sun, C. Thomsen, R.L. Meng, C.W. Chu, Phys. Rev. B 57 (1998) 2872.
- [22] L. Vasiliu-Doloc, J.W. Lynn, A.H. Moudden, A.M. de Leon-Guevara, A. Revcolevschi, J. Appl. Phys. 81 (1997) 5491.
- [23] A. Urushibara, Y. Moritomo, T. Arima, A. Asamitsu, G. Kido, Y. Tokura, Phys. Rev. B 51 (1995) 14103.